# **International Mechanical Engineering Congress and Exposition**

IMECE2022

October 30-November 3, 2022, Columbus, Ohio

IMECE2022-95146

## Jet Formation After Droplet Impact on Microholed Hydrophilic Surfaces

Md Nur E Alam<sup>1</sup> and Hua Tan<sup>1\*</sup>

<sup>1</sup>School of Engineering and Computer Science, Washington State University-Vancouver

14204 NE Salmon Creek Ave., Vancouver, WA 98686, USA

Abstract: Droplet impacts on solid surfaces produce a wide variety of phenomena such as spreading, splashing, jetting, receding, and rebounding. In microholed surfaces, downward jets through the hole can be caused by the high impact inertia during the spreading phase of the droplet over the substrate as well as the cavity collapse during recoil phase of the droplet. We investigate the dynamics of the jet formed through the single hole during the impacting phase of the droplet on a micro-holed hydrophilic substrate. The sub-millimeter circular holes are created on the 0.2 mm-thickness hydrophilic plastic films using a 0.5 mm punch. Great care has been taken to ensure that the millimeter-sized droplets of water dispensed by a syringe pump through a micropipette tip can impact directly over the microholes. A high-speed video photography camera is employed to capture the full event of impacting and jetting. A MATLAB code has been developed to process the captured videos for data analysis. We study the effect of impact velocity on the jet formation including jet velocity, ejected droplet volume, and breakup process. We find that the Weber number significantly affects outcomes of the drop impact and jetting mechanism. We also examine the dynamic contact angle of the contact line during the spreading and the receding phase.

Keywords: Microholed surface, droplet impact, jetting, jet breakup.

#### **NOMENCLATURE:**

- $\beta$  spreading factor
- $\rho$  density of the fluid (kg/m<sup>3</sup>)
- $\sigma$  surface tension of the fluid (mN/m)
- $\mu$  viscosity of the droplet (mPa. s)
- D droplet diameter (mm)
- $l_c$  capillary length (mm)
- L jet height from the substrate (mm)

- r hole radius ( $\mu$ m)
- $r_n$  necking radius (µm)
- t time (ms)
- $t_c$  capillary time (ms)
- $t_p$  time of pinch-off (ms)
- $U_i$  impact velocity (m/s)
- $V_a$  average jet velocity (m/s)
- $V_d$  droplet volume (m<sup>3</sup>)
- $V_i$  volume of ejected fluid through the hole (m<sup>3</sup>)
- We weber number

### 1. INTRODUCTION

The study of droplet impact dynamics and its outcomes can be traced back a century [1–3]. The outcomes of drop impact over a liquid or solid surface include deposition, splashing, jetting, spreading, and many others [4,5]. Due to its ubiquity in many industrial applications including spray cooling [6], additive manufacturing [7], ink-jet printing [8], and natural processes, droplet impact phenomenon has received significant attention from researchers [5,9]. The impact outcomes depend on different parameters, such as impact velocity, the volume of the droplet, the wetting properties and topography of the substrate, and fluid properties (e.g., viscosity and surface tension), etc. [10–12]. Utilization of the high-speed photography has enabled discovery of some rapid events that occur during the droplet impact, such as jetting induced by cavity collapse [13,14].

In recent years, there is a growing interest on the jetting phenomena following drop impact over solid surface of different properties. Bartolo *et al.* [15] showed that when water droplets gently impact on a hydrophobic surface, the droplet shoots out a violent jet at a speed that can be up to 40 times the initial impact speed. Similar jetting phenomenon has been reported on various

types of hydrophobic surfaces [16],[17], [18]. Researchers also carried out the study of droplet impact on microstructured [19,20], microholed [21], and mesh substrate [22–25]. Tsai et al. [26] experimentally investigated drop impact dynamics onto different superhydrophobic surfaces, consisting of regular polymeric micropatterns and rough carbon nanofibers. Siddique et al. [19,20] have studied the droplet impact dynamics over a mircopollered hydrophilic substrate. They have built a regime map to demonstrate the jetting and breakup conditions for the jet formed due to the cavity collapse during the receding phase of the impacted water-glycerol droplet. Asai et al. [27] has studied the jet evolution and mechanism of satellite drop formation. Modak et al. [23] has proposed a novel printing method using the droplet dynamics over a sieve. Ryu et al. [22] conducted droplet impact on a superhydrophobic mesh and proposed the scaling laws for water penetration pressure and the penetration diameter. Su et al. [24] studied the droplet impact on a wire mesh and developed expression for cone angle of dispersion and dispersion diameter. They have also discussed about the diameter and surface area of the satellite droplets ejected from jet breakup. Sun et al. [25] has experimentally studied the spray phenomena for a droplet impacting over a sieve. They have found two mode of water sprays, one is for the collapse of air cavity during the recoil of the droplet and the other is for the impact force of the droplet. Lorenceau and Quéré [21] has discussed the mechanism and outcomes of the drop impact over a single small hole. They have also studied the dependency and scaling of different parameters. Rozhkov et al. [28] has also shown the spreading and growth of a lamella after impacting a drop over a small diameter stainless steel cylinder.

Although good progress has been made in understanding the outcomes of droplet impact on substrates of many holes including mesh and sieve, most research is focused on the effect of hole structure on the atomization process. In fact, droplet impact on a microholed surface can precisely generate a single micron-sized droplet with proper impact velocity, which can be utilized to print patterns on different types of substrates[23]. However, the effect of impact velocity on the size and number of satellite droplets remains not well understood. Therefore, our present study is focused on understanding how impact velocity of the droplet landing over a hydrophilic substrate with a submillimeter hole affects the formation of the jet and satellite microdroplets. The millimeter-sized droplet of water produced from a micro-needle has been carefully placed over the microhole to impact over the substrate keeping the microhole in the center. A high-speed camera has been used to capture pre- and post-events of the droplet impact. A MATLAB code has been developed for processing captured images. In this work, we have studied the effect of variable impact velocity on outcomes of the droplet impact. A regime map has been built to show the conditions for the jet formation. We have analyzed the maximum spreading factor, volume of the ejected jet, and jet breakup process. The scaling laws for the jet growth and breakup have been proposed in the study.

#### 2. EXPERIMENTAL METHOD & DATA PROCESSING:

The experimental setup consists of two major systems: dispensation and high-speed imaging, as shown in Fig. 1. The dispensation system, including a programmable syringe pump (New Era Pump System NE-1000), a pipette tip, a screw mounting column, and a platform for holding the substrate, is used to produce and land the droplet of diameter  $\sim\!2.8$  mm over a microhole on the substrate. The release height of the droplet can be adjusted with the vertical screw column where the pipette tip is mounted. A plastic film of 200  $\mu$ m thickness is used as the substrate. A punch with a diameter  $\sim\!600~\mu$ m is used to create the circular holes with a diameter  $\sim\!600~\mu$ m through the substrate. The plastic substrate is held by a platform of three degrees of freedom using an assembly of high precision stages (i.e., a XY translation stage and a vertical linear stage).

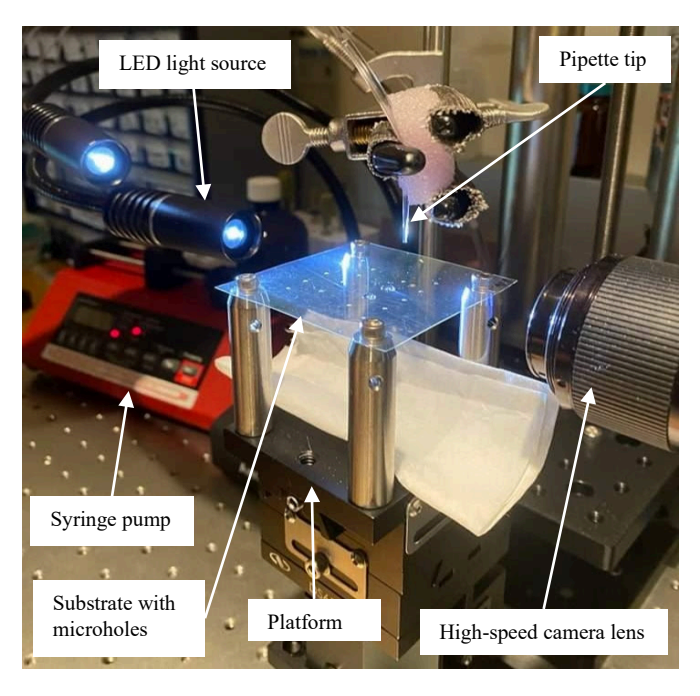


FIGURE 1 EXPERIMENTAL SETUP

In our experiments, the platform is carefully positioned to ensure that the targeted microhole is right beneath the dispensing pipette tip. The Z-position of the platform can be precisely adjusted so that the high-speed camera (a Phantom Miro M310) can properly capture the liquid profile above and below the substrate during droplet impingement. The camera employs a Navitar 12X Zoom Lens. The frame rate of 5638 fps with exposure times of 20 µs is selected. Resulting pixel density is 1280 by 800 pixels. For backlighting, a high-intensity AmScope LED-8WD spotlight is used. The light source and the camera are placed on the opposite side of the substrate so that the light can create a projection of the droplet on the camera. Once the droplet is in range of the camera, an auto-trigger is initiated to capture the subsequent events following droplet impact on the surface. Before and after each experiment, the microholed surface is carefully cleaned with isopropanol, de-ionized water and allowed to dry out completely with the aid of a low temperature hot plate. Each data point gathered from a certain impact velocity and solution is repeated three times to ensure accuracy.

An in-house MATLAB code has been developed to process the large number of captured videos in experiments. For each video, our code can automatically process each frame and output the key results, such as spreading radius, dynamic contact angle, jet height, jet velocity, satellite droplet volume, etc.

In this study, only the impact velocity is varied. The properties of the fluid and substrate remain same for all the cases. Deionized (DI) water is used in the experiments. All the experiments are carried out at room temperature of 22.5°C +/-1°C The viscosity and surface tension of water are 0.96 mPa.s and 72 mN/m respectively. The contact angle of DI water and the plastic substrate is measured as 70° using a digital goniometer.

## 3. RESULT AND DISCUSSION

#### 3.1 Overview

The release height of the droplet varies from 1.0 cm 5.0 cm, resulting in the Weber number ( $We = \rho U_i^2 D/\sigma$ ) in the range from 4.4 to 28. Fig. 2 shows the evolution of jet formation at different impact velocities. It is clear that for all cases, upon impacting the substrate, while the droplet spreads radially over the substrate, it also penetrates through the microhole to form a downward jet. The initial spreading and jetting are caused by the kinetic energy of the droplet. A portion of the kinetic energy is converted to the surface energy after the droplet reaching the maximum spreading above the substrate.

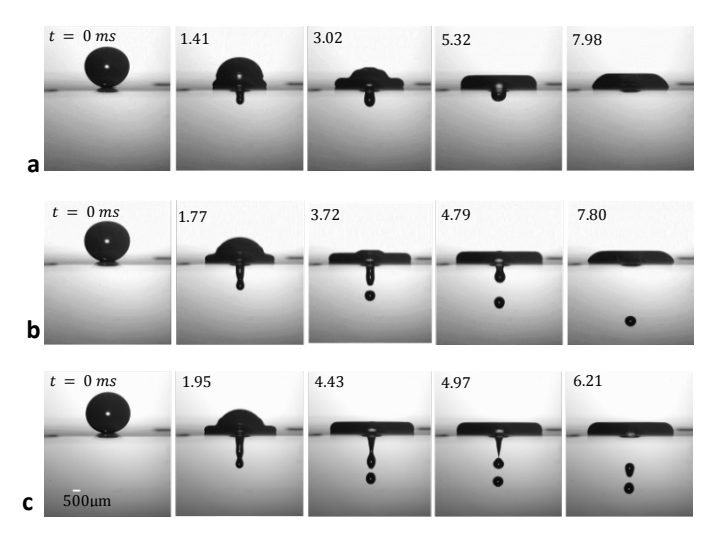


**FIGURE 2** IMAGES OF TYPICAL JETTING EVENT FOR A 100% WATER DROPLET

Sufficient kinetic energy can cause liquid to be ejected below the microhole, which is called "ejected jet" in this work. For We = 10 ( $U_i = 0.5$  m/s), because of insufficient kinetic energy, the initially formed jet retracts under the capillary force and merges with the droplet above the substrate, as shown in Fig. 2 (a). For We = 17 ( $U_i = 0.65$  m/s), as the jet is being stretched through the microhole due to relatively high kinetic energy, the jet tip is growing into a bulb, followed by pinch-off of the bulbous jet tip and ejection of a single satellite droplet, as shown in Fig. 2 (b).

The rest of the jet retracts back to the main droplet through the microhole. For We = 17.83 ( $U_i = 0.67$  m/s), the jet grows faster and longer due to higher inertial force, resulting in multiple breakups of the jet at different times and hence ejection of multiple satellite droplets as shown in Fig. 2 (c). For all the cases involving jet breakup, despite of varing impact velocity, the ejected jet takes a nearly constant time of  $\sim 3.90$  ms to reach to the maximum length and pinch off, suggesting the jet breakup is controlled by the balance between capillary and inertia forces. This breakup time is related to the capillary time scale,  $t_c = (\rho r^3/\sigma)^{1/2}$ .

A regime map of impact outcomes is created to describe the dependency of conditions for breakup on the impact velocity in Fig. 3. There are three separate regimes depending on the breakup conditions. No jet breakup is observed for low impact velocity 0 < We < 10, which is referred to as "no breakup" regime. When the impact velocity exceeds a critical value of  $U_i = 0.51 \, m/s$  (We=10), a single breakup event of the jet occurs and ejects a satellite droplet. So, the 2nd regime 10 < We < 17 is called "single breakup", where a single satellite droplet is ejected due the jet pinch-off. "Multiple breakups" are observed from We = 17 ( $U_i = 0.65 \, m/s$ ) to maximum We limit of our experiments (We = 28). Further experiments need to be performed to know the breakup conditions for higher We.

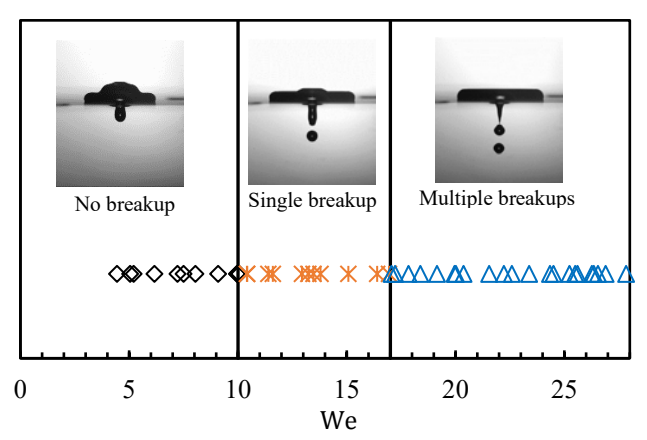
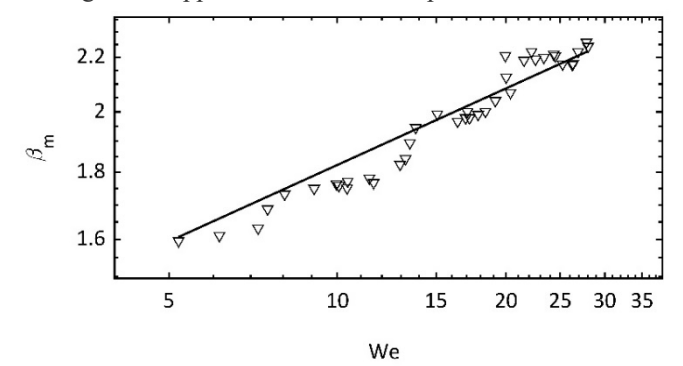


FIGURE 3 REGIME MAP FOR DROPLET IMPACT OVER A MICROHOLED HYDROPHILIC SUBSTRATE

Above the substrate, the droplet deforms into a lamella after reaching the maximum spreading. Then, the droplet starts to recoil due to the surface tension. Various semi-empirical or theoretical models have been developed to predict the maximum spreading factor,  $\beta_{max} = D_{max}/D$  with the maximum spreading diameter  $D_{max}$  for droplet impact on solid surfaces. For inviscid fluid, one would expect full conversion from kinetic energy to surface energy and hence obtain the scaling law  $\beta_{max} \sim We^{0.5}$  by energy conservation. Under the similar capillary dominant condition, Clanet et al. [29] proposed a different scaling law  $\beta_{max} \sim We^{0.25}$  using momentum conservation. If instead the viscous dissipation plays a dominant role during the spreading, the scaling law  $\beta_{max} \sim Re^{0.2}$  (Reynolds number  $Re = \rho U_i D/\mu$  is then expected. We find these scaling laws utilizing We give us the best

fit for our data, as shown in Fig. 4. The solid line in the figure is the power fit of the data with  $R^2 = 0.84$ , i.e.,  $\beta_m \sim We^{0.24}$ . Our study is in good agreement with Clanet *et al.* [29]. Additionally, Laan *et al.* [30] and Tsai *et al.* [31] have also shown the same scaling law is applicable for water droplet.



**FIGURE 4** MAXIMUM SPREADING FACTOR AS A FUNCTION OF WEBER NUMBER

#### 3.2 Jet Evolution

At low impact velocity, jet retracts due to surface tension the maximum length  $L_m$  of the jet is small and no jet pinch-off is observed. In the "no breakup" region, the time to reach  $L_m$  increases with increased We. Our study shows that in the "single breakup" region, the pinch-off time remains constant irrespective of We. In the "multiple breakups" regime, we also find the time to the 1st pinch-off is nearly a constant. Fig. 5 plots the pinch-off time  $t_a$  normalized by the capillary time  $t_c$  against We for all cases. It can be found that  $t_a$  remains nearly constant. Lorenceau and Quéré [21] have also shown that the time of pinch-off is quite independent of the speed of impact, but it strongly depends on the radius of the hole. Similar scaling is found for the upward jetting for droplet impact on super-hydrophobic substrate [32].

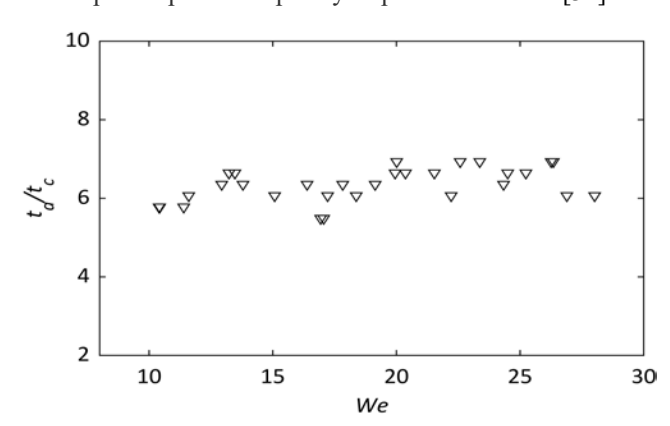


**FIGURE 5** NORMALIZED TIME OF PINCH-OFF WITH WEBER NUMBER

The growth of the downward jet depends on the inertia force of the fluid during impact as well as the supply of fluid through the microhole. We find that the droplet usually reaches to the maximum spreading before the jet is stretched to the maximum length. The inertia force of the fluid above the microhole becomes nearly zero when the droplet spreads most. Then liquid in the jet starts to flow in the upward direction due to surface tension. The

speed of the jet tip is maximum at the beginning when the jet emerges from the microhole. The speed of the jet tip decreases as the jet is being stretched. Our experiments have shown that the average speed  $U_a$  of the jet tip during the period of jet growth is nearly linearly related to the impact velocity  $U_i$  of the droplet, i.e.,  $U_a \sim 2.05U_i$ , as shown in Fig. 6.  $R^2$  of the fitted line is 0.89.

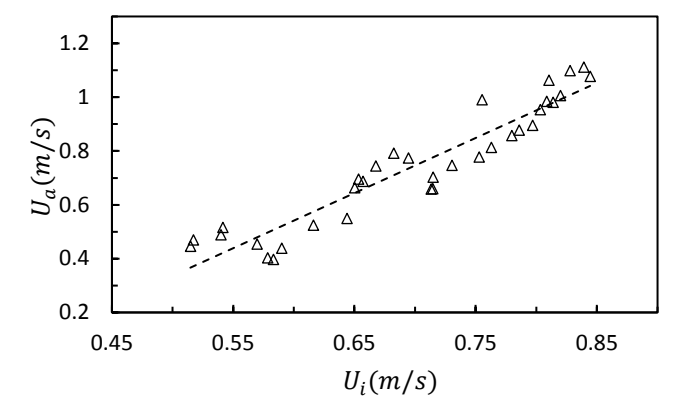


FIGURE 6 AVERAGE VELOCITY OF JET TIP AS A FUNCTION OF IMPACT VELOCITY

The average velocity of the jet tip can be expresses as

$$U_a = L_m/t_a \tag{1}$$

We also can write as,

$$L_m = U_a t_a \tag{2}$$

From the above discussion, we have  $t_a \sim 6.08t_c$  and  $U_a \sim 2.05U_i$ . Now, we can rewrite equation (2) as,

$$L_m \sim 13.1 \, U_i t_c \tag{3}$$

A similar relation has been derived by Lorenceau and Quéré [21]. Fig. 7 plots the maximum jet length  $L_{\rm m}$  before pinch-off versus  $U_i t_c$ . The solid line fitted from the experimental data is  $L_m \sim 13.3 \ U_i t_c$ , which is in very good agreement with equation (3).  $R^2$  of the fitted line is 0.88. Therefore, the impact velocity and capillary time can be used to predict the maximum length of the ejected jet before pinch-off.

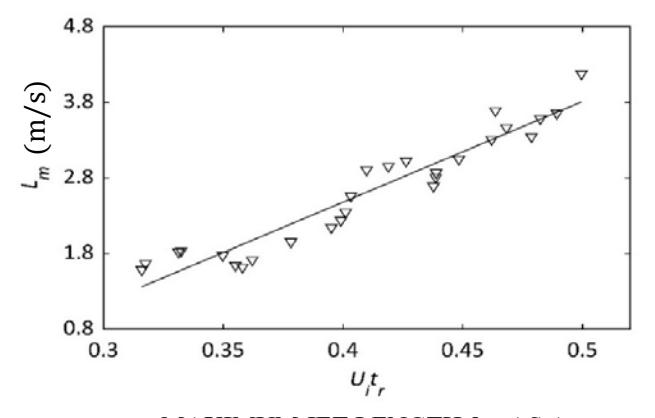


FIGURE 7 MAXIMUM JET LENGTH  $L_m$  AS A FUNCTION OF  $U_it_r$ 

If we approximate the ejected jet of liquid as a cylindrical shape with a diameter equal to that of the microhole, we can estimate the jet volume  $V_i$  by the following equation,

$$V_i = \pi r^2 L_m \tag{4}$$

Replcaing  $L_m$  using equation (3), we have,

$$V_i \sim \pi r^2 U_i t_c \tag{5}$$

If we normalize  $V_j$  by initial droplet volume  $V_d$  and use the Weber number ( $We = \rho U_i^2 D/\sigma$ ), equation (5) can reveal the following scaling law,

$$V_i/Vd \sim We^{0.5} \tag{6}$$

Fig. 8 plots the measured  $V_j$  normalized by  $V_d$  as a function of We. The solid line fitted from experimental data is  $V_j/V_d \sim We^{0.57}$ , which is in good agreement with our scaling analysis.  $R^2$  of the fitted line is 0.89.

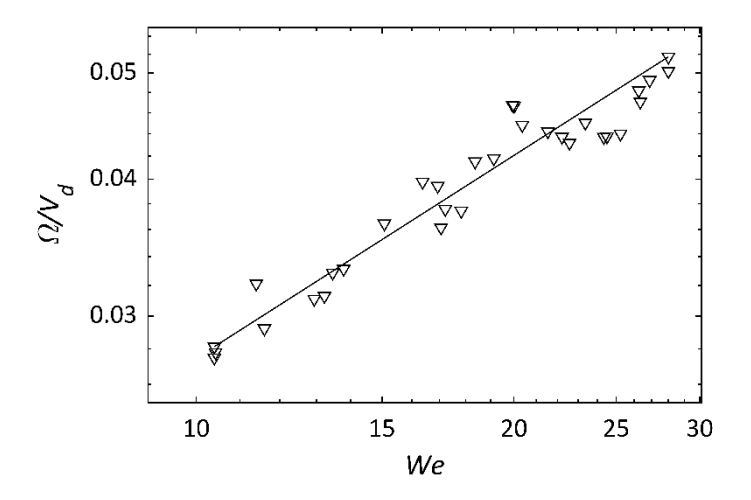


FIGURE 8 EJECTED VOLUME OF LIQUID JET,  $\Omega$  NORMALIZED BY DROPLET VOLUME,  $V_d$  AS A FUNCTION OF WEBER NUMBER

#### 3.3 Breakup of Ejected Jet

The jet observed in our experiments is stretched inertially with the tip gradually growing into a bulb. As the size of the bulbous tip is increasing, necking is found to occur where the jet joins the blob, eventually resulting in the breakup of the jet and emission of satellite droplet. The jet breakup is due to Rayleigh-Plateau instability [37]. Existing studies have shown that the necking radius typically follows a power law with the time to pinch-off. To find the scaling law for the necking process in our experiment, we plot the dimensionless necking radius  $r_n/l_c$  against the dimensionless time  $\tau = (t_b-t)/t_c$  (where  $t_b$  is the time at the moment of jet pinch-off) for a few cases in Fig. 9. We find from the figure that  $r_{\rm n}/l_{\rm c}$  vs.  $\tau$  does follow a power law scaling as  $(r_n/l_c) \sim \tau^{\alpha}$  with  $\alpha = 0.46 \pm 0.03$ .  $R^2$  of the fitted lines varies from 0.93 to 0.96. For low viscosity fluid, the jet breakup is dominated by inertial and capillary forces, leading to the scaling exponent of  $\alpha = 2/3$  [37]. Surprisingly, our scaling exponent is much smaller than the value of 2/3 suggested by scaling theory for inviscid pinch-off. However, it is worth noting that our scaling exponent is close to the case of pinch-off of gas bubble in viscous liquid [33-36].

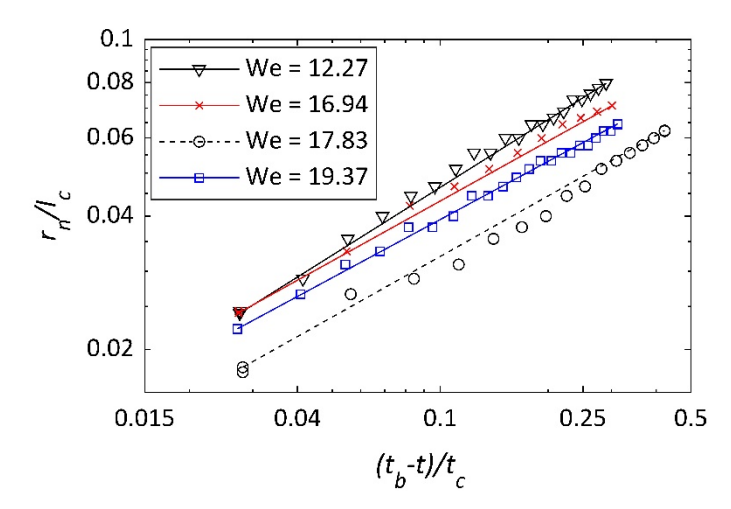


FIGURE 9 NORMALIZED NECKING RADIUS AS A FUNCTION OF NORMALIZED TIME

## 4. CONCLUSION

In this work, we investigate the jet formation of the droplet impacting over a single hole of diameter of 0.6 mm on a hydrophilic substrate. The experiment is performed with DI water for impact velocity ranging from 0.33 m/s to 0.84 m/s. The droplet diameter is kept at 2.86 mm. A high-speed imaging system is employed to capture the entire process of the droplet impact. While the droplet spreads over the substrate upon impact, the liquid also penetrates through the hole to form a jet due to inertial force. The outcome of the jet is significantly affected by the impact velocity. A regime map of the jet outcome is created to convey the dependency of jet dynamics on the Weber number. We find that when impact velocity is lower than the critical velocity of U<sub>i</sub>=0.51 m/s (We=10), no pinch-off of the jet will occur. For  $0.51 \le U_i \le 0.65$  m/s (10 < We < 17), a single jet breakup event occurs, ejecting a satellite droplet. When  $U_i \ge$ 0.65 m/s, the pinch-off of jet occurs multiple times and eject multiple droplets. For the pinch-off process, our data indicate that the radius of the neck reduces with the power law with an exponent of  $\alpha = 0.46 \pm 0.03$ , which is much smaller than the value of 2/3 suggested by scaling analysis for the jet breakup dominated by inertial and capillary forces.

We have also studied the different parameters of the ejected jet. The average velocity of the jet is found to be linearly scaled with the impact velocity. The pinch-off time of the jet (i.e., time period from initialization of jet from the microhole to the moment of pinch-off) is nearly constant and independent of impact velocity, suggesting the pinch-off time is related to the capillary time. Our experimental data shows that the impact velocity and capillary time can be used to approximate the maximum length of the jet. We also find that the volume of the ejected liquid scales

well with  $We^{0.57}$ , which is in close agreement to our scaling analysis  $We^{0.5}$ . Additionally, our experimental data show that the maximum spreading factor of the droplet over the substrate scales with  $We^{0.24}$ , which is in good agreement with existing study.

#### **ACKNOWLEDGEMENT**

The work is funded in part by National Science Foundation Grant CBET-1701339. We also would like to thank the Office of Academic Affairs of WSU- Vancouver for additional financial support.

## REFERENCES

- [1] Worthington, A. M. (Arthur M., 1908, *A Study of Splashes*, London, New York, Bombay, Calcutta: Longmans, Green, and Co.
- [2] Worthington, A. M. (Arthur M., 1895, *The Splash of a Drop*, London, S.P.C.K.
- [3] "III. A Second Paper on the Forms Assumed by Drops of Liquids Falling Vertically on a Horizontal Plate" [Online]. Available: https://royalsocietypublishing.org/doi/epdf/10.1098/rspl.1 876.0073. [Accessed: 18-Apr-2022].
- [4] Yarin, A. L., 2006, "DROP IMPACT DYNAMICS: Splashing, Spreading, Receding, Bouncing...," Annu. Rev. Fluid Mech., **38**(1), pp. 159–192.
- [5] Rioboo, R., Voué, M., Vaillant, A., and De Coninck, J., 2008, "Drop Impact on Porous Superhydrophobic Polymer Surfaces," Langmuir, **24**(24), pp. 14074–14077.
- [6] Breitenbach, J., Roisman, I., and Tropea, C., 2017, "Heat Transfer in the Film Boiling Regime: Single Drop Impact and Spray Cooling," International Journal of Heat and Mass Transfer, 110, pp. 34–42.
- [7] Gilani, N., Aboulkhair, N., Simonelli, M., East, M., Ashcroft, I., and Hague, R., 2022, "From Impact to Solidification in Drop-on-Demand Metal Additive Manufacturing Using MetalJet," Additive Manufacturing, 55, p. 102827.
- [8] van Dam, D. B., and Le Clerc, C., 2004, "Experimental Study of the Impact of an Ink-Jet Printed Droplet on a Solid Substrate," Physics of Fluids, **16**(9), pp. 3403–3414.
- [9] Pasandideh-Fard, M., Qiao, Y. M., Chandra, S., and Mostaghimi, J., 1996, "Capillary Effects during Droplet Impact on a Solid Surface," Physics of Fluids, 8(3), pp. 650–659.
- [10] Moghtadernejad, S., Lee, C., and Jadidi, M., 2020, "An Introduction of Droplet Impact Dynamics to Engineering Students," Fluids, 5(3), p. 107.
- [11] Walls, P., Henaux, L., and Bird, J., 2015, "Jet Drops from Bursting Bubbles: How Gravity and Viscosity Couple to Inhibit Droplet Production," Physical review. E, Statistical, nonlinear, and soft matter physics, **92**, p. 021002.
- [12] Antonini, C., Amirfazli, A., and Marengo, M., 2012, "Drop Impact and Wettability: From Hydrophilic to Superhydrophobic Surfaces," Physics of Fluids, 24(10), p. 102104.

- [13] Thoroddsen, S. T., Etoh, T. G., and Takehara, K., 2008, "High-Speed Imaging of Drops and Bubbles," Annual Review of Fluid Mechanics, **40**(1), pp. 257–285.
- [14] R, R., Saklani, N., and Verma, V., 2019, "A Review on Edge Detection Technique 'Canny Edge Detection," International Journal of Computer Applications, 178, pp. 28–30.
- [15] Bartolo, D., Josserand, C., and Bonn, D., 2006, "Singular Jets and Bubbles in Drop Impact," Phys. Rev. Lett., **96**(12), p. 124501.
- [16] Yamamoto, K., Motosuke, M., and Ogata, S., 2018, "Initiation of the Worthington Jet on the Droplet Impact," Appl. Phys. Lett., **112**(9), p. 093701.
- [17] Pearson, J. T., Maynes, D., and Webb, B. W., 2012, "Droplet Impact Dynamics for Two Liquids Impinging on Anisotropic Superhydrophobic Surfaces," Exp Fluids, 53(3), pp. 603–618.
- [18] Yamamoto, K., Takezawa, H., and Ogata, S., 2016, "Droplet Impact on Textured Surfaces Composed of Commercial Stainless Razor Blades," Colloids and Surfaces A: Physicochemical and Engineering Aspects, 506, pp. 363–370.
- [19] Siddique, A. U., Trimble, M., Zhao, F., Weislogel, M. M., and Tan, H., 2020, "Jet Ejection Following Drop Impact on Micropillared Hydrophilic Substrates," Phys. Rev. Fluids, 5(6), p. 063606.
- [20] Siddique, A. U., Zhao, F., Weislogel, M., and Tan, H., 2020, "Jet Initiation After Drop Impact on Micropatterned Hydrophilic Surfaces," American Society of Mechanical Engineers Digital Collection.
- [21] Lorenceau, É., and Quéré, D., 2003, "Drops Impacting a Sieve," Journal of Colloid and Interface Science, **263**(1), pp. 244–249.
- [22] Ryu, S., Sen, P., Nam, Y., and Lee, C., 2017, "Water Penetration through a Superhydrophobic Mesh During a Drop Impact," Phys. Rev. Lett., 118(1), p. 014501.
- [23] Modak, C. D., Kumar, A., Tripathy, A., and Sen, P., 2020, "Drop Impact Printing," Nat Commun, 11(1), p. 4327.
- [24] Su, M.-J., Luo, Y., Chu, G.-W., Cai, Y., Le, Y., Zhang, L.-L., and Chen, J.-F., 2020, "Dispersion Behaviors of Droplet Impacting on Wire Mesh and Process Intensification by Surface Micro/Nano-Structure," Chemical Engineering Science, 219, p. 115593.
- [25] Sun, L., Lin, S., Pang, B., Wang, Y., Li, E., Zu, X., Zhang, K., Xiang, X., and Chen, L., 2021, "Water Sprays Formed by Impinging Millimeter-Sized Droplets on Superhydrophobic Meshes," Physics of Fluids, 33(9), p. 092111.
- [26] Tsai, P., Pacheco, S., Pirat, C., Lefferts, L., and Lohse, D., 2009, "Drop Impact upon Micro- and Nanostructured Superhydrophobic Surfaces," Langmuir, **25**(20), pp. 12293–12298.
- [27] Asai, B., Siddique, A. U., and Tan, H., 2021, "Jet Dynamics Associated with Drop Impact on Micropillared Substrate," Fluids, 6(4), p. 155.
- [28] Rozhkov, A., Prunet-Foch, B., and Vignes-Adler, M., 2002, "Impact of Water Drops on Small Targets," Physics of Fluids, **14**(10), pp. 3485–3501.

- [29] Clanet, C., Béguin, C., RICHARD, D., and QUÉRÉ, D., 2004, "Maximal Deformation of an Impacting Drop," Journal of Fluid Mechanics, **517**, pp. 199–208.
- [30] Laan, N., Bruin, K., Bartolo, D., Josserand, C., and Bonn, D., 2014, "Maximum Diameter of Impacting Liquid Droplets," Physical Review Applied, 2.
- [31] Tsai, P., Hendrix, M., Dijkstra, R., Shui, L., and Lohse, D., 2011, "Microscopic Structure Influencing Macroscopic Splash at High Weber Number†," Soft Matter, 7.
- [32] Richard, D., Clanet, C., and Quéré, D., 2002, "Contact Time of a Bouncing Drop," Nature, 417(6891), pp. 811– 811.
- [33] Brenner, M., Eggers, J., Joseph, K., Nagel, S., and Shi, X., 1997, "Breakdown of Scaling in Droplet Fission at High Reynolds Number," Physics of Fluids PHYS FLUIDS, 9, pp. 1573–1590.
- [34] Thoroddsen, S. T., Etoh, T. G., and Takehara, K., 2007, "Experiments on Bubble Pinch-Off," Physics of Fluids, 19(4), p. 042101.
- [35] Keim, N. C., Møller, P., Zhang, W. W., and Nagel, S. R., 2006, "Breakup of Air Bubbles in Water: Memory and Breakdown of Cylindrical Symmetry," Phys. Rev. Lett., 97(14), p. 144503.
- [36] Burton, J. C., Waldrep, R., and Taborek, P., 2005, "Scaling and Instabilities in Bubble Pinch-Off," Phys. Rev. Lett., **94**(18), p. 184502.
- [37] J. Eggers and E. Villermaux, Rep. Prog. Phys. **71**, 036601 (2008)